© IWA Publishing 2020
673

Water Practice & Technology Vol 15 No 3
doi: 10.2166/wpt.2020.054

Adsorption dynamics of dye onto crab shell chitosan/neem leaf composite

Asokogene Oluwadayo Francis[a,b], Muhammad Abbas Ahmad Zaini[b,*], Idris Misau Muhammad[c], Surajudeen Abdulsalam[c] and Usman Aliyu El-Nafaty[c]

[a] Department of Mineral and Petroleum Resources Engineering, Federal Polytechnic, Auchi, Edo State, Nigeria

[b] Centre of Lipids Engineering and Applied Research (CLEAR), Ibnu-Sina Institute for Scientific and Industrial Research (ISI-SIR), Universiti Teknologi Malaysia, Johor Bahru, Johor, Malaysia

[c] Department of Chemical Engineering, Abubakar Tafawa Balewa University, Bauchi, Bauchi State, Nigeria

*Corresponding author. E-mail: abbas@cheme.utm.my

Abstract

The aim of this study was to evaluate the adsorption dynamics of crab shell chitosan/neem leaf composite against methylene blue dye at varying concentrations (50 and 200 mg/L), bed depths (2.5 and 5.0 cm), and flow rates (2.17 and 2.90 mL/min). The chitosan composite has a specific surface of 258 m^2/g. Its surface is rich in amine/amide groups. The results reflect better dye adsorption at higher operating conditions. The maximum dye adsorption capacity observed was almost 77 mg/g. The kinetics models showed good correlation with the experimental data and described the breakthrough behaviour of dye removal. The Thomas model predicts external and internal diffusion as the rate controlling mechanisms, while the Adams-Bohart model indicates a simultaneous steady state process of intraparticle diffusion and ionic interaction. Chitosan composite is a promising adsorbent candidate for dye wastewater treatment.

Key words: adsorbent composite, adsorption dynamics, crab shell chitosan, methylene blue dye, neem leaf

Highlights

- Crab shell chitosan/neem leaf composite is mesoporous with a 258 m^2/g specific surface area.
- The removal of dye was improved at high dynamics operating conditions.
- The maximum methylene blue capacity is 77 mg/g.
- External and internal diffusion are the rate controlling mechanisms.

Graphical Abstract

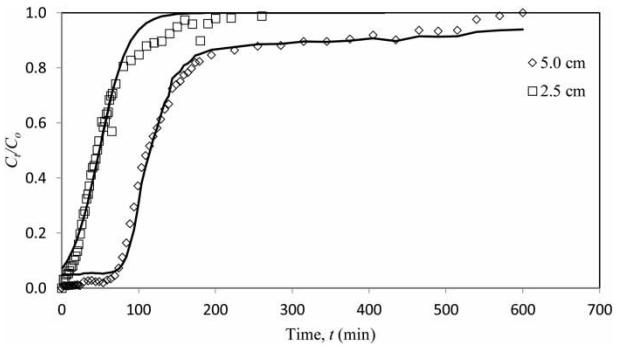

Water Practice & Technology Vol 15 No 3
doi: 10.2166/wpt.2020.054

INTRODUCTION

Dye-containing effluent from paint, leather, textile, pulp and paper industries is a serious ecological concern (Long-Fei *et al.* 2017; Shany & Giora 2018). Most dyes are toxic in water and possibly carcinogenic, and can stay in the environment for a long period (Mehdi *et al.* 2018; Wenjue *et al.* 2018). Such pollutants affect not only aquatic ecosystems, but also human health and the food chain. Methylene blue ($C_{16}H_{18}CIN_3S$) is a typical example of a toxic cationic dye commonly used to dye silk, cotton, and wool (Thakur *et al.* 2016; Miyah *et al.* 2018). For that reason, environmental protection agencies have listed methylene blue among the priority pollutants to be removed from water streams (Hameed & Rahman 2008; Jia & Lua 2008).

Several conventional methods are available in wastewater treatment for removing methylene blue, these includes ion exchange, precipitation, biodegradation, ozone treatment, membrane filtration, photocatalysis, coagulation, flocculation, oxidation and adsorption (Aysan *et al.* 2016; Rajasulochana & Preethy 2016; Luo *et al.* 2017; Wang *et al.* 2017). These methods often have high operating and maintenance costs, and special handling for hazardous by-products disposal (Tabari *et al.* 2012). Among them, adsorption is favoured because it is relatively cheap, simple and easy to operate, and effective in removing low concentration pollutants (Aysan *et al.* 2016; Lakshmi *et al.* 2016; Pathania *et al.* 2017; Tahir *et al.* 2017; Apurva *et al.* 2018).

The development of a natural, low-cost adsorbent for methylene blue has become increasingly attractive (Annaduzzaman 2015). Auta & Hameed (2012) reported methylene blue removal of 160, 298 and 377 mg/g at concentrations of 50, 100 and 200 mg/L, respectively, using waste tea activated carbon/chitosan composite beads in a column with 3.6 cm bed thickness and 5 mL/min flow rate. Makrigianni *et al.* (2017) reported the performance of acid-treated, pyrolytic tyre char as 2.08, 3.79 and 3.85 mg/g at concentrations of 10, 20 and 40 mg/L, respectively, in a 15 cm tall column operating at 100 mL/min. Similarly, Auta & Hameed (2014) showed methylene blue adsorption onto chitosan/clay composite of 142 mg/g, at a concentration of 200 mg/L in a 3.6 cm bed at 5 mL/min flow rate.

Modified chitosan has gained wide attention as an effective adsorbent due to its versatility in water, especially when blended with a robust material to form a composite (Li & Tang 2016). Modified chitosan contains high concentrations of amino and hydroxyl functional groups that have significant affinity for positively charged water pollutants (Zdarta *et al.* 2015; Tondwal & Singh 2018). As far as is known, however, no work has been done to date on methylene blue adsorption by crab shell chitosan/neem leaf composite (chitosan composite) in column-mode. Crab shell and neem leaves are available at little cost as primary sources for chitosan composite and offer a new alternative to current adsorbents. Therefore, this study was aimed at assessing the adsorption dynamics of chitosan composite on methylene blue removal. The dynamics of the column-mode process were analysed and described using the Adams-Bohart, Thomas and Yoon-Nelson models.

MATERIALS AND METHODS

Materials

Crab shell and neem leaves were obtained from Auchi, Nigeria. All chemicals used were of analytical grade: sodium hydroxide pellets (99%, Merck, Germany), hydrochloric acid (37%, Fisher Scientific, USA), oxalic acid pellets (99%, Merck, Germany) and methylene blue powder (98.5% Merck, Germany).

Synthesis and characterization of the chitosan composite

Crab shell was deproteinised, demineralised and deacetylised to produce chitosan, from which the 300 μm material was screened (Asokogene *et al.* 2019). Neem leaves were rinsed with distilled water, oven-dried at 110 °C for 150 minutes, ground to a fine powder and heat-treated in a muffle furnace at

Water Practice & Technology Vol 15 No 3
doi: 10.2166/wpt.2020.054

250 °C for 180 minutes. Thirty grams of chitosan was mixed with 10% (w/v) oxalic acid solution, and stirred for 1 hour at 50 °C and 200 rpm, before 50 g of powdered neem leaf was added slowly, stirred continuously for 2 hours and allowed to stand for 24 hours. The chitosan composite was removed from the solution and washed with distilled water. Next, it was soaked in 0.5% (w/v) sodium hydroxide solution for 3 hours. Finally, the material was rinsed with distilled water and dried in an oven at 110 °C.

The chitosan composite was characterized for textural properties using a Micromeritics ASAP 2010 analyzer, and surface chemistry using a Nicolet ISI 10 Fourier transform infrared (FTIR) spectrometer (both Thermo Scientific, USA).

Adsorption dynamics

Adsorption in continuous mode was carried out in a 56.7 cm tall, 0.75 cm inner diameter column. The chitosan composite was packed into the column at bed depths of 2.5 cm (0.5 g) and 5.0 cm (1.0 g). Steel mesh was placed above and below, to prevent material loss and allow uniform solution flow. Methylene blue concentrations of 50 and 200 mg/L were used to challenge the composite at up-flow rates of 2.17 and 2.90 mL/min. The solution was pumped upward to avoid channelling due to gravity in the adsorption bed. The treated dye solution was collected regularly at the column top, and the dye concentration was determined using a UV-Vis spectrophotometer (DU 8200, Drawell Scientific, China) at 620 nm. The experiment was carried out at room temperature (30 °C) and natural pH (4.8 $\pm$ 0.3). The breakthrough curve showing the mass transfer zone was established from the plot of C_t/C_o against t (min), where C_t and C_o are the effluent and influent concentrations, and t the service time (Afroze *et al.* 2016). The influent concentration and flow rate were varied, and the removal capacity was determined from the area under the plot by integrating the amount of methylene blue adsorbed, expressed as C_{ads}, where $C_{ads} = C_o - C_t$ at time t. The amount of methylene blue adsorbed in the column, q_{total} (mg), was calculated using Equation (1) (Yagub *et al.* 2014):

$$q_{total} = \frac{QA}{1000} = \frac{Q}{1000} \int_{t=0}^{t=t_{total}} C_{ad} dt \tag{1}$$

where t_{total} (min), Q (mL/min) and A are the total flow time, volumetric flow rate and area under the breakthrough curve, respectively. Equilibrium uptake, $q_{o,eq}$ (mg/g), was determined using Equation (2).

$$q_{o.eq} = \frac{q_{total}}{m} \tag{2}$$

where m (g) is the adsorbent weight in the column. The amount of methylene blue passed through the column, M_{total} (mg), was determined using Equation (3).

$$M_{total} = \frac{C_o Q t_{total}}{1000} \tag{3}$$

The percentage of methylene blue removed is the quotient of the maximum capacity of the column, q_{total}, divided by the total amount of methylene blue sent to the column, M_{total} – Equation (4):

$$Total\ removal = \frac{q_{total}}{M_{total}} \times 100 \tag{4}$$

At equilibrium, the methylene blue concentration, C_{eq} (mg/g), in the continuous flow system is expressed in Equation (5):

$$C_{eq} = \frac{M_{total} - q_{total}}{V_{eff}} \times 1000 \tag{5}$$

and the effluent volume, V_{eff} (mL), in Equation (6):

$$V_{eff} = Q \times t_{total} \tag{6}$$

Water Practice & Technology Vol 15 No 3
doi: 10.2166/wpt.2020.054

RESULTS AND DISCUSSION

Adsorbent characteristics

The chitosan composite has a specific surface of 258 m^2/g, with 65.4% mesoporosity and mean pore diameter of 2.07 nm. The FTIR spectrum of chitosan composite shows an absorption band at 3,679–3,332 cm^{-1}, corresponding to O – H hydrogen bond and N – H stretching vibrations of primary and secondary amine/amide groups in the material (Asokogene *et al.* 2019).

Methylene blue adsorption dynamics

Figures 1–3 show the effect of operating conditions on column-mode methylene blue adsorption onto chitosan composite as presented in breakthrough curves. The column parameters are summarized in Table 1.

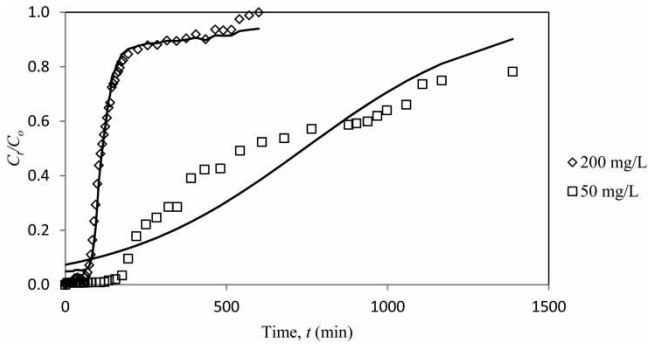

Figure 1 | Methylene blue adsorption breakthrough curves using chitosan composite at 50 and 200 mg/L concentrations (flow rate = 2.17 mL/min, bed thickness = 5.0 cm, lines predicted by the Adams-Bohart model).

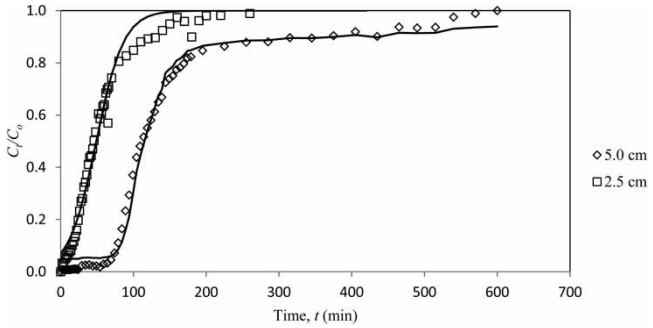

Figure 2 | Methylene blue adsorption breakthrough curves for different bed thicknesses (flow rate = 2.17 mL/min, concentration = 200 mg/L, lines predicted by the Adams-Bohart model).

The effect of adsorbate concentration on dye adsorption under fixed conditions – flow rate 2.17 mL/min, bed thickness 5.0 cm and pH 4.8 ± 0.3 – is presented in Figure 1. The breakthrough curve remains close to the abscissa for 155 minutes for influent concentration 50 mg/L. At 200 mg/L, a shorter breakthrough time of 64 minutes was observed. Accordingly, a throughput of 3,012 mL can be treated at the lower dye concentration. The values of q_{total} and M_{total} increased from 55.6 to 63.3 mg, and 122 to 238 mg, respectively, with the increase in dye concentration, while the removal efficiency decreased from 45.6 to 26.6% due to the higher residual concentration in the column effluent. A similar dynamic pattern was reported by López-Cervantes *et al.* (2018).

Water Practice & Technology Vol 15 No 3
doi: 10.2166/wpt.2020.054

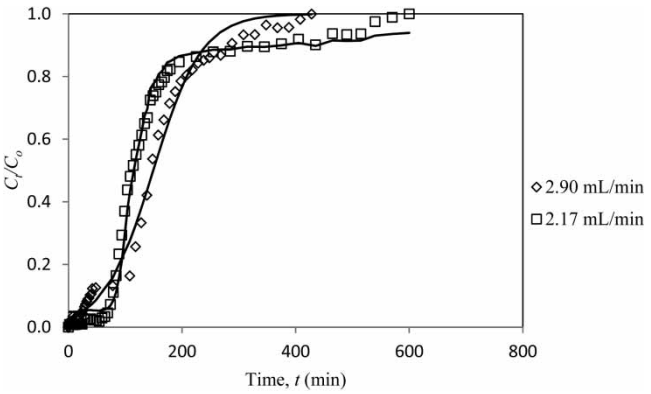

Figure 3 | Methylene blue adsorption breakthrough curves at different flow rates (bed thickness = 5.0 cm, inlet concentration = 200 mg/L, lines predicted by the Adams-Bohart model).

Table 1 | Column-mode parameters for methylene blue adsorption onto chitosan composite under different operating conditions

Bed thickness (cm)	C_o (mg/L)	Q (mL/min)	q_{total} (mg)	M_{total} (mg)	V_{eff} (ml)	Removal efficiency (%)	$q_{o,eq}$ (mg/g)	C_{eq} (mg/L)
2.50	200	2.17	19.2	162	911	11.8	38.4	157
5.00	200	2.17	63.3	238	1,302	26.6	63.3	134
5.00	200	2.90	76.8	227	1,241	33.8	76.8	121
5.00	50	2.17	55.6	122	3,012	45.6	55.6	22.0

The operation embraced the difference in solute mass transfer because of the concentration gradient between 50 and 200 mg/L (Karimi *et al.* 2012; López-Cervantes *et al.* 2018). The adsorbent was exhausted after 1,108 and 195 min for the 50 and 200 mg/L influents, respectively.

The effect of bed thickness on methylene blue adsorption dynamics at $C_o = 200$ mg/L is shown in Figure 2. Increasing the bed thickness from 2.5 to 5.0 cm increased the adsorption capacity from 38.4 to 63.3 mg/g. The greater thickness provided numerous active sites and more residence time for adsorbent-adsorbate interaction, thereby increasing adsorption capacity (López-Cervantes *et al.* 2018).

Figure 3 shows the effect of flow rate on methylene blue adsorption dynamics. Adsorption was rapid at both flow rates, possibly due to the abundance of vacant active sites and ionic interactions. As adsorption continued, there was a reduction in the adsorption rate as more sites were occupied (Afroze *et al.* 2016). An adsorption capacity of 76.8 mg/g was recorded at 2.90 mL/min flow rate, suggesting the prevalence of mass transfer and protonation of amine groups at higher flow rates in promoting dye molecule diffusion onto chitosan composite (Auta & Hameed 2012).

Dynamics model fitting

Three dynamics models – Thomas, Yoon-Nelson and Adams-Bohart – were fitted to the experimental data. The Thomas model embraces the mass transfer of solute through a liquid film to the adsorbent surface as its principal transport mechanism. The Yoon-Nelson model depends on the assumption that the rate of decrease in the probability of adsorption is proportional to the probability of adsorption of the dye and breakthrough on the adsorbent composite. The Adams-Bohart model involves the assumption that the adsorption rate is proportional to the adsorbent's residual concentration and the concentration of the adsorbing species. The models

Water Practice & Technology Vol 15 No 3
doi: 10.2166/wpt.2020.054

are presented in Equations (7)–(9), respectively (Makrigianni *et al.* 2017).

$$\frac{C_t}{C_o} = \frac{1}{1 + exp\left(\frac{K_{Th} q_T m}{Q} - K_{Th} C_o t\right)} \tag{7}$$

$$\frac{C_t}{C_o} = \frac{1}{1 + e^{K_{YN}(\tau - t)}} \tag{8}$$

$$\frac{C_t}{C_o} = \frac{1}{1 + exp\left(\frac{K_{BA} N Z}{u} - K_{BA} C_o t\right)} \tag{9}$$

where:

- K_{Th} (mL/min. mg) is the Thomas rate constant, q_T (mg/g) the equilibrium capacity, m (g) the mass of adsorbent, and t (min) the time;
- K_{YN} (min^{-1}) is the Yoon-Nelson rate constant, τ (min) the time required for 50% adsorbate breakthrough; and,
- k_{AB} (L/mg.min) is the Adams-Bohart rate constant, u (cm/min) the linear velocity, Z (cm) the bed thickness, N the maximum adsorption capacity, C_o the influent concentration and C_t the adsorption concentration at time, t.

The column-mode parameters from these models were solved by non-linear regression using MS Excel, and the values are summarized in Table 2.

Generally, the adsorption dynamics data fitted well into all models as reflected in the high correlation of determination (R^2) values, hence their applicability in describing the breakthrough data. The Thomas model analysis shows a decreasing rate constant (K_{TH}) from 0.204 to 0.128 mL/min.mg, with increasing flow rate from 2.17 to 2.90 mL/min, while the equilibrium capacity, q_T, increased from 47.7 to 79.2 mg/g. Similarly, increasing the bed thickness from 2.5 to 5.0 cm caused K_{TH} to decrease from 0.298 to 0.204 mL/min.mg and q_T to increase from 37.7 to 47.7 mg/g. These results signify that the adsorbate residence time in the column and solute mass transfer onto the active sites was sufficient. Therefore, methylene blue adsorption onto chitosan composite increased at higher flow rate, greater bed thickness and lower influent concentration. Similar results were reported by others (Altufaily *et al.* 2019; Talib *et al.* 2018). Generally, the breakthrough simulation for all operating conditions studied obeyed the Thomas model, as indicated by the close agreement of q_T with experimental q_o.

The Yoon-Nelson model shows that increasing the flow rate and bed thickness reduces the rate constant, K_{YN}, and increases the time required for 50% breakthrough. Increasing the influent concentration, however, increases K_{YN} and reduces τ, suggesting increased competition for adsorption sites and higher adsorption capacity (Afroze *et al.* 2016; Altufaily *et al.* 2019).

The Adams-Bohart model shows that the rate constant, K_{AB}, decreases and the saturation concentration, N_o, increases with increasing flow rate and bed thickness. However, increasing influent concentration increases both K_{AB} and N_o, suggesting that the kinetics are concentration driven. Talib *et al.* (2018) reported similar results.

Table 3 is a comparison of methylene blue adsorption by chitosan composite with other adsorbents in column-mode operation from selected literature sources at varying influent concentrations and flow rates. Generally, the chitosan composite displays a competitive performance with the adsorbents listed in Table 3. The ready availability of the natural resources for the chitosan composite and its excellent adsorption potential render it a promising low-cost alternative for dye wastewater treatment.

Water Practice & Technology Vol 15 No 3
doi: 10.2166/wpt.2020.054

Table 2 | Dynamic constants for column-mode operation with methylene blue

			Thomas model				Yoon-Nelson model				Adams-Bohart model			
Influent conc. (mg/L)	**Flow rate (mL/min)**	**Bed thickness (cm)**	K_{TH} **(mL/min.mg)**	q_T**(mg/g)**	**SSE**	R^2	K_{YN} **(min^{-1})**	τ **(min)**	**SSE**	R^2	K_{AB} **(L/mg.min)**	N **(mg/L)**	**SSE**	R^2
200	2.17	2.5	0.298	37.71	0.128	0.984	0.053	48.82	0.128	0.984	2.98×10^{-4}	1.96×10^{4}	0.128	0.984
200	2.17	5.0	0.204	47.65	0.198	0.986	0.037	120.0	0.198	0.986	1.72×10^{-4}	1.98×10^{4}	0.077	0.992
200	2.90	5.0	0.128	79.20	0.067	0.992	0.023	149.2	0.067	0.992	1.28×10^{-4}	4.11×10^{4}	0.067	0.992
50	2.17	5.0	0.086	64.39	0.329	0.904	0.003	741.9	0.329	0.904	8.56×10^{-5}	3.34×10^{4}	0.329	0.904

Water Practice & Technology Vol 15 No 3
doi: 10.2166/wpt.2020.054

Table 3 | Comparison of methylene blue sorption capacity by various adsorbents in column-mode operation

Adsorbent	C_o (mg/L)	Flow rate (mL/min)	Adsorption capacity, q_o (mg/g)	References
Waste tea activated carbon/chitosan composite beads	50	5	128	Auta & Hameed (2012)
	50	5	160	
	50	5	163	
	50	8	197	
	50	10	195	
	100	5	298	
	200	5	377	
Acid-treated pyrolytic tyre char	10	50	1.48	Makrigianni *et al.* (2017)
	10	100	2.08	
	10	150	2.17	
	20	50	2.47	
	20	100	3.79	
	20	150	3.68	
	40	50	2.99	
	40	100	3.85	
	40	150	3.74	
Rice husk ash	20	10	5.33	Kang-Kang *et al.* (2015)
Rice husk/$CoFe_2O_4$ composite	20	10	16.3	Kang-Kang *et al.* (2015)
Waste-derived activated carbon	100	5	7.0	Sarici-Ozdemir (2014)
Chitosan/clay composite	200	5	142	Auta & Hameed (2014)
Crab shell chitosan/neem leaf composite	200	2.17	39.4	This study
	200	2.17	63.3	
	200	2.90	76.8	
	50	2.17	55.6	

CONCLUDING REMARKS

A chitosan composite was used to study methylene blue adsorption dynamics. The mesoporous adsorbent has a specific surface of 258 m^2/g and its performance with respect to methylene blue was comparable to that of other adsorbents reported in literature. Adsorption capacity was affected noticeably by column operating conditions, specifically influent concentration, bed thickness and flow rate. The maximum adsorption capacity recorded was almost 77 mg/g at $C_o = 200$ mg/L. The breakthrough behaviour reveals the importance of external and internal diffusion, and a simultaneous steady-state process of intraparticle diffusion and possibly ionic interaction as the rate controlling mechanisms.

ACKNOWLEDGEMENT

This work was supported by Tertiary Education Trust Fund (TETFund) of Nigeria through an Academic Staff Training and Development (AST&D) grant, and the Ministry of Education of Malaysia and Universiti Teknologi Malaysia through Fundamental Research Grant Scheme (FRGS) No. 4F995.

CONFLICT OF INTEREST

The authors of this work have no conflict of interest to declare.

Water Practice & Technology Vol 15 No 3
doi: 10.2166/wpt.2020.054

DATA AVAILABILITY STATEMENT

All relevant data are included in the paper or its Supplementary Information.

REFERENCES

Afroze, S., Sen, T. K. & Ang, H. M. 2016 Adsorption performance of continuous fixed bed column for the removal of methylene blue (MB) dye using Eucalyptus sheathiana bark biomass. *Research on Chemical Intermediates* **42**(3), 2343–2364.

Altufaily, M. A. M., Nesrin, J. A. & Alaq, F. M. A. 2019 Mathematical modeling of fixed-bed columns for the adsorption of methylene blue onto fired clay pot. *International Journal of ChemTech Research* **12**(2), 70–80.

Annaduzzaman, M. 2015 Chitosan biopolymer as an adsorbent for drinking water treatment-investigation on arsenic and uranium. *TRITA-LWR LIC* **2015**, 2–26.

Apurva, A. N., Fernandes, J. B. & Tilve, S. G. 2018 Adsorption behavior of methylene blue on glycerol based carbon materials. *Journal of Environmental Chemical Engineering* **6**(2), 1714–1725.

Asokogene, O. F., Zaini, M. A. A., Idris, M. M., Abdulsalam, S. & Usman, A. E. 2019 Physicochemical properties of oxalic acid-modified chitosan/neem leave composites from Pessu river crab shell. *International Journal of Chemical Reactor Engineering* **20180274**, 1–12.

Auta, M. & Hameed, B. H. 2012 Coalesced chitosan activated carbon composite for batch and fixed-bed adsorption of cationic and anionic dyes. *Colloids and Surfaces B: Biointerfaces* **105**, 199–206.

Auta, M. & Hameed, B. H. 2014 Chitosan-clay composite as highly effective and low-cost adsorbent for batch and fixed-bed adsorption of methylene blue. *Chemical Engineering Journal* **37**, 352–361.

Aysan, H., Edebali, S., Ozdemir, C., Karakaya, M. C. & Karakaya, N. 2016 Use of chabazite, a naturally abundant zeolite, for the investigation of the adsorption kinetics and mechanism of methylene blue dye. *Microporous and Mesoporous Materials* **235**, 78–86.

Hameed, B. H. & Rahman, A. A. 2008 Removal of phenol from aqueous solutions by adsorption onto activated carbon prepared from biomass material. *Journal of Hazardous Materials* **160**, 576–581.

Jia, Q. & Lua, A. C. 2008 Effects of pyrolysis conditions on the physical characteristics of oil-palm-shell activated carbons used in aqueous phase phenol adsorption. *Journal of Analytical Applied Pyrolysis* **83**, 175–179.

Kang-Kang, Y., Jiao, H., Xue-Gang, C., Shu-Ting, L., Ao-Bo, Z., Ying, Y., Mei, L. & Xiaosheng, J. 2015 Fixed-bed adsorption of methylene blue by rice husk and rice husk/$CoFe_2O_4$ nanocomposite. *Desalination and Water Treatment* **57**(27), 1–11.

Karimi, M., Shojaei, A., Nematollahzadeh, A. & Abdekhodaie, M. J. 2012 Column study of Cr(VI) adsorption onto modified silica-polyacrylamide microspheres composite. *Chemical Engineering Journal* **210**, 280–288.

Lakshmi, S., Harshitha, M., Vaishali, G., Keerthana, S. R. & Muthappa, R. 2016 Studies on different methods for removal of phenol in wastewater – review. *International Journal of Science, Engineering and Technology Research* **5**(7), 2488–2496.

Li, X. Q. & Tang, R. C. 2016 Cross-linked and dyed chitosan fiber presenting enhanced acid resistance and bioactivities. *Polymers (Basel)* **8**, 119.

Long-Fei, R., Rui, C., Xiaofan, Z., Shao, J. & He, Y. 2017 Phenol biodegradation and microbial community dynamics in extractive membrane bioreactor (EMBR) for phenol-laden saline wastewater. *Journal of Bioresource Technology* **244**, 1121–1128.

López-Cervantes, J., Sánchez-Machado, D. I., Sánchez-Duarte, R. G. & Correa-Murrieta, M. A. 2018 Study of a fixed-bed column in the adsorption of an azo dye from an aqueous medium using a chitosan–glutaraldehyde biosorbent. *Adsorption Science and Technology* **36**(1–2), 215–232.

Luo, X. P., Fu, S. Y., Du, Y. M., Guo, J. Z. & Li, B. 2017 Adsorption of methylene blue and malachite green from aqueous solution by sulfonic acid group modified MIL-101. *Microporous and Mesoporous Materials* **237**, 268–274.

Makrigianni, V., Giannakas, A., Hela, D., Papadaki, M. & Konstantinou, I. 2017 Adsorption of methylene blue dye by pyrolytic tire char in fixed bed column. *Desalination and Water Treatment* **65**, 346–358.

Mehdi, M., Mohammad, A. A., Peyman, S., Yousefi, M., Nazari, M. & Brask, J. 2018 Immobilization of laccase on epoxy-functionalized silica and its application in biodegradation of phenolic compounds. *International Journal of Biological Macromolecules* **109**, 443–447.

Miyah, Y., Lahrichi, A., Idrissi, M., Khalil, A. & Zerrouq, F. 2018 Adsorption of methylene blue from aqueous solutions onto walnut shells powder: equilibrium and kinetic studies. *Surfaces and Interfaces* **11**, 74–81.

Pathania, D., Sharma, S. & Singh, P. 2017 Removal of methylene blue by adsorption onto activated carbon developed from Ficus carica bast. *Arabian Journal of Chemistry* **10**, 1445–1451.

Rajasulochana, P. & Preethy, V. 2016 Comparison on efficiency of various techniques in treatment of waste and sewage water – a comprehensive review. *Resource Efficient Technologies* **2**, 175–184.

Sarici-Ozdemir, C. 2014 Removal of methylene blue by activated carbon prepared from waste in a fixed-bed column. *Particulate Science and Technology* **32**, 311–318.

Shany, B. M. & Giora, R. 2018 Thiamine-based organo-clay for phenol removal from water. *Journal of Applied Clay Science* **155**, 50–56.

Water Practice & Technology Vol 15 No 3
doi: 10.2166/wpt.2020.054

Tabari, T., Tavakkoli, H., Zargaran, P. & Beiknejad, D. 2012 Fabrication of Perovskite type oxide bapbo$_3$ nanoparticles and their efficiency in photodegradation of methylene blue. *South African Journal of Chemistry* **65**, 239–244.

Tahir, N., Bhatti, H. N., Iqbal, M. & Noreen, S. 2017 Biopolymers composites with peanut hull waste biomass and application for Crystal Violet adsorption. *International Journal of Biological Macromolecules* **94**, 210–220.

Talib, M. I., Chauhan, Y. P. & Parate, V. R. 2018 *Packed bed Adsorption Study on Phenol Removal and its Modeling*. Available from: http://www.researchgate.net/publication/322757361 (accessed 14 July 2019).

Thakur, S., Pandey, S. & Arotiba, O. A. 2016 Development of a sodium alginate-based organic/inorganic superabsorbent composite hydrogel for adsorption of methylene blue. *Carbohydrate Polymers* **153**, 34–46.

Tondwal, R. & Singh, M. 2018 Chitosan functionalization with a series of sulfur-containing α-amino acids for the development of drug-binding abilities. *Journal of Applied Polymer Science* **135**(12), 46000.

Wang, F., Zhang, L., Wang, Y., Liu, X., Rohani, S. & Lu, J. 2017 Fe_3o_4@SiO_2@CS-TETA functionalized graphene oxide for the adsorption of methylene blue (MB) and Cu(II). *Applied Surface Science* **420**, 970–981.

Wenjue, Z., Donghong, W. & Zijian, W. 2018 Distribution and potential ecological risk of 50 phenolic compounds in three rivers in Tianjin, China. *Journal of Environmental Pollution* **235**, 121–128.

Yagub, M., Sen, T., Afroze, S. & Ang, H. 2014 Dye and its removal from aqueous solution by adsorption: a review. *Advances in Colloid and Interface Science Journal* **209**, 172–184.

Zdarta, J., Klapiszewski, L., Wysokowski, M., Norman, M., Kolodziejczak-Radzimska, A., Moszynski, H., Ehrlich, H., Maciejewski, A., Sterling, D. & Jesionowski, T. 2015 Chitin-lignin material as a novel matrix for enzyme immobilization. *Marine Drugs* **13**(4), 2424–2446.